The nuclear to cytoplasmic ratio directly regulates zygotic transcription in *Drosophila*

Henry Wilky[1], Sahla Syed[2], João Raimundo[1], Bomyi Lim[2]*, and Amanda A. Amodeo[1]*

1 Lewis-Sigler Institute for Integrative Genomics, Princeton University
2 Department of Chemical and Biomolecular Engineering, University of Pennsylvania
*Corresponding authors: Bomyi Lim (bomyilim@seas.upenn.edu) and Amanda Amodeo (aamodeo@princeton.edu)

Summary:
Early embryos must rapidly generate large numbers of cells to form an organism. Many species accomplish this through a series of rapid, reductive, and transcriptionally silent cleavage divisions. Previous work has demonstrated that before both cell cycle elongation and zygotic genome activation (ZGA), the number of divisions is regulated by the ratio of nuclear content to cytoplasm (N/C). To understand how the N/C ratio affects the timing of ZGA we directly assayed the behavior of several previously identified N/C-ratio-dependent genes using the MS2-MCP reporter system in living *Drosophila* embryos with altered ploidy and cell cycle time. For every gene that we examined, we found that transcription is delayed in haploids. The N/C ratio influences transcription through two separate modes of action. For many genes the effect of ploidy can be entirely accounted for by changes in cell cycle duration. However, for a subset of genes the N/C ratio directly affects the probability of transcription initiation. While it appears that cell cycle duration is the dominant component in modulating transcription for most genes, our data demonstrate that the regulatory elements of at least some genes respond directly to the N/C-ratio, independent of interphase length.

Key words: Zygotic genome activation, ZGA, Maternal to zygotic transition, MZT, Mid-blastula transition, MBT, transcription, developmental timing, haploids, Chk1

Introduction:

The early embryo of many fast, externally developing species is largely transcriptionally silent during the rapid cleavage stage preceding a developmental transition known as the midblastula transition (MBT) (Newport and Kirschner, 1982a,b). At the MBT, the cell cycle slows and major zygotic genome activation (ZGA) occurs (Schulz and Harrison, 2019; Vastenhouw et al., 2019; Lefebvre and Lecuyer, 2018; Liu and Grosshans, 2017; Jukam et al., 2017; Yuan et al., 2016; Blythe and Wieschaus, 2015a; Harrison and Eisen, 2015). The timing of both cell cycle slowing and ZGA are controlled by the ratio of nuclear material, likely DNA, to cytoplasm (N/C ratio), as seen from previous studies that used manipulations in ploidy, injection of exogenous DNA, removal of cytoplasm, or changes in cell size to alter this ratio (Figure 1A) (Newport and Kirschner, 1982a; Edgar et al., 1986; Almouzni and Wolffe, 1995; Lee et al., 2001; Dekens et al., 2003; Lu et al., 2009; Jevtic and Levy, 2015; Chen et al., 2019; Chan et al., 2019)

Since transcription and the cell cycle are tightly coupled, disentangling which is upstream during the MBT has remained difficult (Jukam et al., 2017; Ferree et al., 2016). On the one hand, transcript accumulation is necessarily dependent on the length of the transcriptional window, i.e. interphase duration (Shermoen and O'Farrell, 1991; Rothe et al., 1992; Yuan et al., 2016). Indeed, artificial manipulation of the cell cycle results in corresponding changes to the timing of ZGA in frogs, fish, and flies (Edgar and Schubiger, 1986; Kimelman et al., 1987; Collart et al., 2013; Chan et al., 2019; Strong et al., 2017), and pharmacological inhibition of transcription does not affect cell cycle behavior in frogs or fish (Newport and Dasso, 1989; Clute and Masui,

1995; Hadzhiev et al., 2019; Müller et al., 2001). In *Drosophila* and zebrafish, it has been observed that the majority of the early transcripts are short and lack introns, leading to the suggestion that the early interphases simply are not long enough to sustain robust transcription of most genes (McKnight and Miller, 1976; Shermoen and O'Farrell, 1991; Rothe et al., 1992; De Renzis et al., 2007; Chen et al., 2013; Heyn et al., 2014; Kwasnieski et al., 2019). On the other hand, ZGA has been implicated as upstream of cell cycle slowing. Premature activation of transcription does lead to early cell cycle slowing in flies, while transcription inhibition leads to its delay (in contrast to frogs and fish) (Sung et al., 2013; Edgar and Datar, 1996; Shermoen et al., 2010). In flies, zygotic transcripts such as *fruhstart* (*frs* or *z600*) and *tribbles* are known to directly regulate core cell cycle components (Grosshans and Wieschaus, 2000; Grosshans et al., 2003; Di Talia et al., 2013; Farrell and O'Farrell, 2013; Sung et al., 2013). In addition, the association of RNA-polymerase with DNA has been proposed to cause replication stress which activates the DNA damage checkpoint to slow the cell cycle (Blythe and Wieschaus, 2015b).

Given this complex interdependence between the cell cycle and transcription, the question of whether the effect of N/C ratio on transcription is direct or indirect has remained open (Figure 1B). *In vitro*, at least one transcript is directly sensitive to the N/C ratio in cell cycle arrested *Xenopus* egg extracts, but it is unclear if this direct relationship is maintained *in vivo* for any or all genes (Amodeo et al., 2015). *In vivo*, manipulations in ploidy coupled with RNA-seq, microarrays, or qPCR have found that haploid *Drosophila, Xenopus*, and zebrafish embryos have reduced gene expression when compared to their wild type counterparts with a spectrum of N/C-dependence across transcribed genes (Lu et al., 2009; Jevtić and Levy, 2017; Chan et al., 2019;). However, these experiments are ill suited to determine if the observed changes in transcription are a direct response to the altered N/C ratio or an indirect response to changes in cell cycle duration because they lack the temporal resolution required to properly account for the cumulative changes in interphase length. Moreover, experiments that examine endogenous genes in ploidy manipulated embryos are inherently confounded by the effect that ploidy has on template availability. Whole embryo sequencing based approaches also destroy the spatial information within an embryo which is important since many of the early genes are spatially patterned. Fixed tissue imaging-based approaches such as *in situ* hybridization or labeled ribonucleotide incorporation can avoid the latter problem, but also lack the temporal resolution required to fully address if and how transcriptional dynamics respond to the N/C ratio.

In this study, we have employed the MS2-MCP system to directly and quantitatively investigate the effects of the N/C ratio on real-time transcriptional dynamics in the early *Drosophila* embryo. This system allows us to follow the transcription of candidate genes over the course of several cell cycles with <30 second temporal resolution. We find that for all of the genes studied, N/C-ratio-dependent changes in interphase duration result in proportional changes in total transcription output within a given cycle. For the majority of genes studied, even those that had previously been classified as N/C-ratio dependent, we find no direct effect of ploidy on the number of transcribing nuclei or activation kinetics suggesting that their regulation is downstream of cell cycle changes. However, for the cell cycle regulator *frs*, we find that the timing of transcription activation is directly dependent on the N/C ratio, such that fewer nuclei are activated in haploids of the same cycle. Therefore, we conclude that while all genes are affected by the N/C ratio through cell cycle duration, a subset of genes including *frs* contain regulatory elements that respond directly to the N/C ratio.

Results:

Total transcriptional output is sensitive to N/C ratio

First, we sought to characterize the transcriptional dynamics of previously categorized N/C-ratio-dependent and N/C-ratio-independent genes during the *Drosophila* early cycles in response to changes in ploidy (Lu et al 2009). Since *Drosophila* forgo cytokinesis until the MBT when the resulting syncytium is cellularized, these first 13 divisions are referred to as nuclear cycles (NCs, not to be confused with the N/C ratio). We used the *sesame/Hira185b* (*ssm185b*) mutation to prevent sperm chromatin decondensation and generate haploid embryos (referred to hereafter as haploids) (Loppin et al., 2000, 2001, 2005). The cycle lengths of these haploid embryos are shifted by precisely one nuclear cycle (e.g., duration of diploid NC13 = haploid NC14) and undergo one additional nuclear division in order to reach the same N/C ratio (where N is proportional to the total amount of DNA, not number of nuclei) as their diploid counterparts (Figure 1A) (Edgar et al., 1986; Lu et al., 2009, Di Talia et al., 2013; Farrell and O'Farrell, 2013; Blythe and Wieschaus, 2016; Shindo and Amodeo, 2019). We visualized nascent transcription in the developing embryo through the MS2-MCP system (Bertrand et al., 1998; Forrest and Gavis, 2003; Golding et al., 2005; Larson et al., 2011; Garcia et al., 2013). When the inserted 24 MS2 repeats are transcribed the nascent RNA is bound by MCP:GFP, resulting in a fluorescence signal that is directly proportional to transcription output (Garcia et al., 2013; Fukaya et al., 2016). Thus, this system provides a sensitive and high-resolution live readout of transcriptional activity. To remove the confounding effects of copy number on transcriptional output we compared wild-type (WT) embryos that were heterozygous for a given MS2 construct to haploids which also only contained a single copy (see Method Details). This platform allows us to directly measure the effects of the N/C ratio on transcription fully controlled for both cell cycle time and template availability.

Since we were interested in the features that underlie N/C ratio sensitivity we chose three genes that had been previously identified as N/C-ratio-dependent (*knirps*, *giant*, and *fruhstart*) and one N/C-ratio-independent gene (*snail*) for our analysis (Lu et al 2009; Fukaya et al., 2016). We found that *knirps* (*kni*) and *giant* (*gt*) have broadly similar behavior and therefore focus on *kni* as an example N/C-dependent gene and *sna* as an example N/C-independent gene (Figure S1A and S1C). To confirm that transcription is delayed in haploids, we measured the total amount of mRNA production for each nuclear cycle from NC10 to NC14 (or NC15 for haploid). We found that for all of the genes that we studied, including the N/C-independent gene *snail* (*sna*), the cumulative output of each haploid cycle appears to be delayed by precisely one cycle as compared to WT (Figure 2A and 2B, Figure S1), consistent with previous reports of transcriptional delays in embryos with reduced ploidy, but inconsistent with the previous N/C ratio-dependent or time-dependent categorizations (Lu et al., 2009). To understand the underlying cause of this change in transcriptional output, we plotted average fluorescent signal across all transcribing nuclei over time (Figure 2C and 2D, Figure 4G, Figure S2C). For all genes, we observed premature termination of transcription in the shortened haploid cycles which explains much of the difference in total per nucleus output (Figure 2C and 2D, Fig S2C). Indeed, when fluorescent signal is aligned by equivalent N/C ratio, and therefore cell cycle duration (e.g. WT NC13 and haploid NC14), the transcriptional trajectories of haploid and WT better align (Figure 2E and 2F, Figure S2D). These findings suggest that N/C-ratio-dependent changes in the duration of the transcriptional window may underlie the observed changes in total output within a cell cycle, however they do not rule out additional direct N/C ratio dependent effects.

<u>The N/C ratio modulates transcriptional output through control of the cell cycle</u>

Next, we sought to more deeply investigate the possibility of direct N/C-ratio-dependent effects on the transcriptional machinery. If the regulatory elements of a given gene are directly sensing the N/C ratio we would expect effects on polymerase loading, transcription initiation, or the rate of elongation independent of the observed effects of cell cycle duration. These differences would manifest in changes in the kinetics of the MS2 reporter such as the timing of first MS2 detection, maximum amplitude of transcriptional signal, and/or the initial slope of activation (Figure 3A). To examine the kinetics of initial transcriptional activation we measured the transcriptional output in the first 2.5 minutes after transcriptional initiation, which includes only the rising phase for all samples (Fig 3D and 3E). We find the output in the first 2.5 minutes for *kni, gt, frs,* and *sna* transcriptional activity are consistent between WT and haploids within all haploid and WT cell cycles (Figure 3D and 3E, Figure 4E, Figure S2B). We note that both genotypes display a small increase in the initial output with age, consistent with transcriptional memory or increased translation of transcriptional activators (Ferraro et al., 2016; Foo et al., 2014; Yamada et al., 2019). From this we conclude that the kinetics of initial transcriptional activation are not sensitive to the N/C ratio (Figure 3D and 3E). In contrast, we found that the maximum amplitude of the MS2 signal within a given cell cycle was, in fact, reduced in haploids as compared to WT for *kni, gt, frs,* and *sna* (Figure S3). However, since the signal in the early cycles never reaches steady state, we reasoned that the shortened cell cycle may be responsible for this observation due to premature truncation during the rising phase (Figure 2C-F).

Since the shorter cell cycle in haploids makes it difficult to disentangle the effect of cell cycle duration versus N/C-ratio on transcription, we compared haploids to diploid embryos with similarly shortened cell cycles produced by mutation of checkpoint kinase 1 (*grp*/*chk1*, referred to hereafter as short-cycle diploid) (Blythe and Wieschaus, 2015b; Fogarty et al., 1994; Sibon et al., 1997). These embryos die after NC13 and therefore cannot be analyzed further. Unsurprisingly, the duration of active transcription scales directly with cell cycle duration for all genes (Fig 3B and 3C, Figure S2A). As predicted, we found the maximum amplitude achieved within a cycle was indistinguishable between short-cycle-diploids and haploid for *kni*, *frs* and *sna* (Figure S3A, S3C, and S3D). Additionally, we found that the output in the first 2.5 minutes was unchanged in short-cycle-diploids (Figure 3D and 3E). This indicates that the small change in the maximum amplitude observed between WT and haploid can be attributed to changes in cell cycle duration or cell cycle state, not changes in the underlying competency of the transcription machinery. Indeed, when matched by nuclear cycle the short-cycle-diploids and haploid average trajectories are nearly identical despite the two-fold difference in ploidy (Figure 2F and 2G). Therefore, the N/C ratio does not directly affect any observable transcriptional parameter within those nuclei that activate for all of the genes in our study.

The regulatory elements of a subset of genes respond directly to the N/C ratio

While the N/C ratio does not affect the slopes or maximum amplitudes of transcription of transcribing nuclei for any of the genes that we assayed, the N/C ratio could also alter the probability that a nucleus ever initiates transcription at all within a cycle. In this case, we would expect that the number of nuclei that become transcriptionally active at any point during the cell cycle would be reduced in haploids as compared to WT. It is important to note that ploidy does not change the total number of nuclei in a given cycle, only the amount of DNA in each nucleus (Figure 4A-D, Figure S4). We found that for the majority of genes that we studied (*kni*, *gt*, and *sna*) the total number of transcribing nuclei was indistinguishable between haploids and WT (Figure 4A and C, Figure S4). In fact, for these genes the total number of nuclei that transcribe at any point approximately doubles with each cycle in both genotypes, indicating that the

percent of nuclei transcribing is relatively constant for *kni*, *gt*, and *sna* throughout the syncytial blastoderm cycles (Figure 4C, Figure S4). This result highlights the gradual, non-switch-like nature of transcription activation of many early zygotic genes (Edgar and Schubiger, 1986; Pritchard and Schubiger, 1996).

However, one gene, the cell cycle regulator *frs*, was directly N/C ratio sensitive in its probability of transcriptional activation. *frs* is a ubiquitously expressed cyclin-CDK1 inhibitor, which is involved in cell cycle slowing at the MBT (Grosshans et al., 2003; Lu et al., 2009; Gawliński et al., 2007). Unlike the steady progression observed in other genes that we examined, *frs* activation is highly switchlike with only 16% of nuclei active in WT NC12 jumping to 80% in WT NC13 (Figure 4D). Moreover, we found the switch from majority inactive to majority active nuclei was delayed by precisely one cell cycle in haploids (Figure 4B and 4D). After haploid NC14, *frs* is fully activated and the number of nuclei actively transcribing doubles to the total number of nuclei in haploid NC15, as we observed in the other genes (Figure 4D). Critically, the number of active nuclei were comparable in NC13 between WT and in short-cycle-diploids (Figure 4D), demonstrating that the switch-like activation of *frs* is a direct effect of ploidy, independent of cell cycle duration.

A similar pattern is displayed when comparing the total per nucleus output of *frs* in active nuclei to that of the other genes in this study that is highly reflective of cell cycle duration in both haploids and short-cycle-diploids (Figure 4F and 4G, Figure S1D). The initial slope of transcription initiation in those nuclei that do initiate in the earlier cycles is unaffected by ploidy (Figure 4E and 4G). These results indicate that the regulatory elements of *frs* are directly responsive to the N/C ratio in a binary on/off fashion and that the N/C ratio has no detectable additional effect on transcription kinetics.

Discussion:

Here we have shown that the total transcriptional output during the MBT is a function of the N/C ratio for several zygotic genes in *Drosophila* regardless of their previous categorization. For these genes, the primary, and many cases only, effect is due to N/C-dependent changes in the length of the transcriptional window. This results in less total mRNA production within a given cycle due to the abortion of transcription at mitosis (Shermoen and O'Farrell, 1991; Rothe et al., 1992; Djabrayan et al., 2019; Kwasnieski et al., 2019). However, for at least one gene, *frs*, transcriptional activation is directly sensitive to the N/C ratio. *frs* is uniquely switch-like in our study, which may be a consequence of its responsiveness to the exponentially increasing N/C ratio (Figure 4B and 4D). This process may set a threshold for the recruitment of polymerase to, or more likely, release from pausing at the *frs* promoter. The promoter of *frs*, as well as the other genes we assayed, are already nucleosome-free by NC11 indicating chromatin opening alone cannot explain their differences in timing (Blythe and Wieschaus, 2016). Nonetheless, *frs* is responsive to experimental alterations in histone availability which is decreasing over the course of the early divisions (Wilky et al., 2019; Shindo and Amodeo, 2019). This is in contrast to the other zygotic genes that do not respond directly to the N/C ratio (*sna*, *kni*, and *gt*) which also have limited histone sensitivity (Wilky et al., 2019).

In addition to its switch like behavior, *frs* is unique in our gene set as a cell cycle regulator, while the others are developmental patterning genes. Frs protein binds and inhibits cyclins to slow the cell cycle (Gawliński et al., 2007). Therefore, the finding that *frs* transcription directly responds to the N/C ratio places it in an excellent position to be the primary N/C ratio sensor that couples transcription to the cell cycle (Grosshans and Wieschaus, 2000; Grosshans et al., 2003). However, *frs* transcription alone cannot explain the entire phenomenon of N/C-ratio-dependent

cell cycle slowing as only a small percentage of *frs* mutant embryos show defects in this process (Grosshans et al., 2003). Therefore, other N/C-ratio-sensitive transcripts, or transcription independent N/C ratio sensing mechanisms must be involved. Here, another putative N/C-ratio-sensitive cell cycle regulator, *tribbles* is an excellent candidate and will require further study to determine its ability to directly respond to the N/C ratio (Grosshans and Wieschaus, 2000; Farrell and O'Farrell, 2013).

We also note that most manipulations of the N/C ratio are, in fact, manipulations in ploidy. In these cases, we speculate the transcript accumulation is much more dramatically affected than the simple response to N/C-ratio-dependent cell cycle duration since the amount of template for a given transcript would be halved. Template reduction could also directly affect the process of cell cycle slowing. For example, in the proposed model where RNA-polymerase on the DNA acts as the source of replication stress, simply halving the amount of DNA without changing other aspects of transcription would halve the number of such conflicts embryo-wide (Blythe and Wieschaus, 2015b). This may permit an additional cell cycle in haploids to allow for the critical number of global conflicts to induce the checkpoint response to slow the cell cycle. Our findings suggest that this may be the dominant mode of action since the majority of genes do not appear to directly respond to the N/C ratio. Additionally, they constrain the available models for how the N/C ratio influences both the cell cycle and transcription, directly or indirectly. In sum, we have demonstrated that the N/C ratio regulates all zygotic transcription in *Drosophila* by shortening the cell cycle with a subset of genes exhibiting additional upstream regulation through N/C-ratio dependent modulation of the probability of transcription initiation.

Acknowledgments:
We are grateful to Gary Laevsky and the Molecular Biology Confocal Imaging Facility and Gordon Gray and the *Drosophila* Media Core Facility at Princeton University for technical support. We thank Michal Levo for reagents. We thank Eric Wieschaus, Stas Shvartsman, and Mike Levine for discussion. Stocks obtained from the Bloomington *Drosophila* Stock Center (NIH P40OD018537) were used in this study. BL is supported by NIH R35GM133425.

References:

Almouzni, G., Wolffe, A.P., 1995. Constraints on transcriptional activator function contribute to transcriptional quiescence during early Xenopus embryogenesis. EMBO J. 14, 1752–1765.

Amodeo, A.A., Jukam, D., Straight, A.F., Skotheim, J.M., 2015. Histone titration against the genome sets the DNA-to-cytoplasm threshold for the *Xenopus* midblastula transition. Proceedings of the National Academy of Sciences 112, E1086–E1095. https://doi.org/10.1073/pnas.1413990112

Bertrand, E., Chartrand, P., Schaefer, M., Shenoy, S.M., Singer, R.H., Long, R.M., 1998. Localization of ASH1 mRNA particles in living yeast. Mol. Cell 2, 437–445.

Blythe, S.A., Wieschaus, E.F., 2016. Establishment and maintenance of heritable chromatin structure during early Drosophila embryogenesis. eLife 5. https://doi.org/10.7554/eLife.20148

Blythe, Shelby A., Wieschaus, E.F., 2015. Coordinating Cell Cycle Remodeling with Transcriptional Activation at the Drosophila MBT, in: Current Topics in Developmental Biology. Elsevier, pp. 113–148. https://doi.org/10.1016/bs.ctdb.2015.06.002

Blythe, Shelby A., Wieschaus, E.F., 2015. Zygotic Genome Activation Triggers the DNA Replication Checkpoint at the Midblastula Transition. Cell 160, 1169–1181. https://doi.org/10.1016/j.cell.2015.01.050

Chan, S.H., Tang, Y., Miao, L., Darwich-Codore, H., Vejnar, C.E., Beaudoin, J.-D., Musaev, D., Fernandez, J.P., Benitez, M.D.J., Bazzini, A.A., Moreno-Mateos, M.A., Giraldez, A.J.,

2019. Brd4 and P300 Confer Transcriptional Competency during Zygotic Genome Activation. Developmental Cell 49, 867-881.e8. https://doi.org/10.1016/j.devcel.2019.05.037

Chen, H., Einstein, L.C., Little, S.C., Good, M.C., 2019. Spatiotemporal Patterning of Zygotic Genome Activation in a Model Vertebrate Embryo. Developmental Cell 49, 852-866.e7. https://doi.org/10.1016/j.devcel.2019.05.036

Chen, K., Johnston, J., Shao, W., Meier, S., Staber, C., Zeitlinger, J., 2013. A global change in RNA polymerase II pausing during the Drosophila midblastula transition. eLife 2, e00861. https://doi.org/10.7554/eLife.00861

Clute, P., Masui, Y., 1995. Regulation of the Appearance of Division Asynchrony and Microtubule-Dependent Chromosome Cycles in Xenopus laevis Embryos. Developmental Biology 171, 273–285. https://doi.org/10.1006/dbio.1995.1280

Collart, C., Allen, G.E., Bradshaw, C.R., Smith, J.C., Zegerman, P., 2013. Titration of four replication factors is essential for the Xenopus laevis midblastula transition. Science 341, 893–896. https://doi.org/10.1126/science.1241530

De Renzis, S., Elemento, O., Tavazoie, S., Wieschaus, E.F., 2007. Unmasking Activation of the Zygotic Genome Using Chromosomal Deletions in the Drosophila Embryo. PLoS Biol 5, e117. https://doi.org/10.1371/journal.pbio.0050117

Dekens, M.P.S., Pelegri, F.J., Maischein, H.-M., Nüsslein-Volhard, C., 2003. The maternal-effect gene futile cycle is essential for pronuclear congression and mitotic spindle assembly in the zebrafish zygote. Development 130, 3907–3916.

Di Talia, S., She, R., Blythe, S.A., Lu, X., Zhang, Q.F., Wieschaus, E.F., 2013. Posttranslational Control of Cdc25 Degradation Terminates Drosophila's Early Cell-Cycle Program. Current Biology 23, 127–132. https://doi.org/10.1016/j.cub.2012.11.029

Djabrayan, N.J.-V., Smits, C.M., Krajnc, M., Stern, T., Yamada, S., Lemon, W.C., Keller, P.J., Rushlow, C.A., Shvartsman, S.Y., 2019. Metabolic Regulation of Developmental Cell Cycles and Zygotic Transcription. Current Biology 29, 1193-1198.e5. https://doi.org/10.1016/j.cub.2019.02.028

Edgar, B.A., Datar, S.A., 1996. Zygotic degradation of two maternal Cdc25 mRNAs terminates Drosophila's early cell cycle program. Genes & Development 10, 1966–1977. https://doi.org/10.1101/gad.10.15.1966

Edgar, B.A., Kiehle, C.P., Schubiger, G., 1986. Cell cycle control by the nucleo-cytoplasmic ratio in early Drosophila development. Cell 44, 365–372. https://doi.org/10.1016/0092-8674(86)90771-3

Edgar, B.A., Schubiger, G., 1986. Parameters controlling transcriptional activation during early Drosophila development. Cell 44, 871–877. https://doi.org/10.1016/0092-8674(86)90009-7

Farrell, J.A., O'Farrell, P.H., 2013. Mechanism and Regulation of Cdc25/Twine Protein Destruction in Embryonic Cell-Cycle Remodeling. Current Biology 23, 118–126. https://doi.org/10.1016/j.cub.2012.11.036

Ferraro, T., Esposito, E., Mancini, L., Ng, S., Lucas, T., Coppey, M., Dostatni, N., Walczak, A.M., Levine, M., Lagha, M., 2016. Transcriptional Memory in the Drosophila Embryo. Current Biology 26, 212–218. https://doi.org/10.1016/j.cub.2015.11.058

Ferree, P.L., Deneke, V.E., Di Talia, S., 2016. Measuring time during early embryonic development. Seminars in Cell & Developmental Biology 55, 80–88. https://doi.org/10.1016/j.semcdb.2016.03.013

Fogarty, P., Kalpin, R.F., Sullivan, W., 1994. The Drosophila maternal-effect mutation grapes causes a metaphase arrest at nuclear cycle 13. Development 120, 2131–2142.

Foo, S.M., Sun, Y., Lim, B., Ziukaite, R., O'Brien, K., Nien, C.-Y., Kirov, N., Shvartsman, S.Y., Rushlow, C.A., 2014. Zelda Potentiates Morphogen Activity by Increasing Chromatin Accessibility. Current Biology 24, 1341–1346. https://doi.org/10.1016/j.cub.2014.04.032

Forrest, K.M., Gavis, E.R., 2003. Live Imaging of Endogenous RNA Reveals a Diffusion and Entrapment Mechanism for nanos mRNA Localization in Drosophila. Current Biology 13, 1159–1168. https://doi.org/10.1016/S0960-9822(03)00451-2

Fukaya, T., Lim, B., Levine, M., 2016. Enhancer Control of Transcriptional Bursting. Cell 166, 358–368. https://doi.org/10.1016/j.cell.2016.05.025

Garcia, H.G., Tikhonov, M., Lin, A., Gregor, T., 2013. Quantitative Imaging of Transcription in Living Drosophila Embryos Links Polymerase Activity to Patterning. Current Biology 23, 2140–2145. https://doi.org/10.1016/j.cub.2013.08.054

Gawliński, P., Nikolay, R., Goursot, C., Lawo, S., Chaurasia, B., Herz, H.-M., Kussler-Schneider, Y., Ruppert, T., Mayer, M., Grosshans, J., 2007. The Drosophila mitotic inhibitor Frühstart specifically binds to the hydrophobic patch of cyclins. EMBO Rep. 8, 490–496. https://doi.org/10.1038/sj.embor.7400948

Golding, I., Paulsson, J., Zawilski, S.M., Cox, E.C., 2005. Real-time kinetics of gene activity in individual bacteria. Cell 123, 1025–1036. https://doi.org/10.1016/j.cell.2005.09.031

Gratz, S.J., Ukken, F.P., Rubinstein, C.D., Thiede, G., Donohue, L.K., Cummings, A.M., O'Connor-Giles, K.M., 2014. Highly Specific and Efficient CRISPR/Cas9-Catalyzed Homology-Directed Repair in *Drosophila*. Genetics 196, 961–971. https://doi.org/10.1534/genetics.113.160713

Grosshans, J., Müller, H.A.J., Wieschaus, E., 2003. Control of cleavage cycles in Drosophila embryos by frühstart. Dev. Cell 5, 285–294.

Großhans, J., Wieschaus, E., 2000. A Genetic Link between Morphogenesis and Cell Division during Formation of the Ventral Furrow in Drosophila. Cell 101, 523–531. https://doi.org/10.1016/S0092-8674(00)80862-4

Hadzhiev, Y., Qureshi, H.K., Wheatley, L., Cooper, L., Jasiulewicz, A., Van Nguyen, H., Wragg, J.W., Poovathumkadavil, D., Conic, S., Bajan, S., Sik, A., Hutvàgner, G., Tora, L., Gambus, A., Fossey, J.S., Müller, F., 2019. A cell cycle-coordinated Polymerase II transcription compartment encompasses gene expression before global genome activation. Nature Communications 10. https://doi.org/10.1038/s41467-019-08487-5

Harrison, M.M., Eisen, M.B., 2015. Transcriptional Activation of the Zygotic Genome in Drosophila, in: Current Topics in Developmental Biology. Elsevier, pp. 85–112. https://doi.org/10.1016/bs.ctdb.2015.07.028

Heyn, P., Kircher, M., Dahl, A., Kelso, J., Tomancak, P., Kalinka, A.T., Neugebauer, K.M., 2014. The Earliest Transcribed Zygotic Genes Are Short, Newly Evolved, and Different across Species. Cell Reports 6, 285–292. https://doi.org/10.1016/j.celrep.2013.12.030

Jevtić, P., Levy, D.L., 2017. Both Nuclear Size and DNA Amount Contribute to Midblastula Transition Timing in Xenopus laevis. Sci Rep 7, 7908. https://doi.org/10.1038/s41598-017-08243-z

Jevtić, P., Levy, D.L., 2015. Nuclear Size Scaling during Xenopus Early Development Contributes to Midblastula Transition Timing. Current Biology 25, 45–52. https://doi.org/10.1016/j.cub.2014.10.051

Jukam, D., Shariati, S.A.M., Skotheim, J.M., 2017. Zygotic Genome Activation in Vertebrates. Developmental Cell 42, 316–332. https://doi.org/10.1016/j.devcel.2017.07.026

Kimelman, D., Kirschner, M., Scherson, T., 1987. The events of the midblastula transition in Xenopus are regulated by changes in the cell cycle. Cell 48, 399–407. https://doi.org/10.1016/0092-8674(87)90191-7

Kwasnieski, J.C., Orr-Weaver, T.L., Bartel, D.P., 2019. Early genome activation in *Drosophila* is extensive with an initial tendency for aborted transcripts and retained introns. Genome Res. 29, 1188–1197. https://doi.org/10.1101/gr.242164.118

Larson, D.R., Zenklusen, D., Wu, B., Chao, J.A., Singer, R.H., 2011. Real-time observation of transcription initiation and elongation on an endogenous yeast gene. Science 332, 475–478. https://doi.org/10.1126/science.1202142

Lee, D.R., Lee, J.E., Yoon, H.S., Roh, S.I., Kim, M.K., 2001. Compaction in preimplantation mouse embryos is regulated by a cytoplasmic regulatory factor that alters between 1- and 2-cell stages in a concentration-dependent manner. Journal of Experimental Zoology 290, 61–71. https://doi.org/10.1002/jez.1036

Lefebvre, F., Lécuyer, É., 2018. Flying the RNA Nest: Drosophila Reveals Novel Insights into the Transcriptome Dynamics of Early Development. JDB 6, 5. https://doi.org/10.3390/jdb6010005

Lim, B., Heist, T., Levine, M., Fukaya, T., 2018. Visualization of Transvection in Living Drosophila Embryos. Molecular Cell 70, 287-296.e6. https://doi.org/10.1016/j.molcel.2018.02.029

Liu, B., Grosshans, J., 2017. Link of Zygotic Genome Activation and Cell Cycle Control. Methods Mol. Biol. 1605, 11–30. https://doi.org/10.1007/978-1-4939-6988-3_2

Loppin, B., Berger, F., Couble, P., 2001. The Drosophila maternal gene sésame is required for sperm chromatin remodeling at fertilization. Chromosoma 110, 430–440. https://doi.org/10.1007/s004120100161

Loppin, B., Bonnefoy, E., Anselme, C., Laurençon, A., Karr, T.L., Couble, P., 2005. The histone H3.3 chaperone HIRA is essential for chromatin assembly in the male pronucleus. Nature 437, 1386–1390. https://doi.org/10.1038/nature04059

Loppin, B., Docquier, M., Bonneton, F., Couble, P., 2000. The Maternal Effect Mutation sésame Affects the Formation of the Male Pronucleus in Drosophila melanogaster. Developmental Biology 222, 392–404. https://doi.org/10.1006/dbio.2000.9718

Lu, X., Li, J.M., Elemento, O., Tavazoie, S., Wieschaus, E.F., 2009. Coupling of zygotic transcription to mitotic control at the Drosophila mid-blastula transition. Development 136, 2101–2110. https://doi.org/10.1242/dev.034421

McKnight, S.L., Miller Jr., O.L., 1976. Ultrastructural patterns of RNA synthesis during early embryogenesis of Drosophila melanogaster. Cell 8, 305–319. https://doi.org/10.1016/0092-8674(76)90014-3

Müller, F., Lakatos, L., Dantonel, J., Strähle, U., Tora, L., 2001. TBP is not universally required for zygotic RNA polymerase II transcription in zebrafish. Curr. Biol. 11, 282–287. https://doi.org/10.1016/s0960-9822(01)00076-8

Newport, J., Dasso, M., 1989. On the coupling between DNA replication and mitosis. Journal of Cell Science 1989, 149–160. https://doi.org/10.1242/jcs.1989.Supplement_12.13

Newport, J., Kirschner, M., 1982a. A major developmental transition in early xenopus embryos: I. characterization and timing of cellular changes at the midblastula stage. Cell 30, 675–686. https://doi.org/10.1016/0092-8674(82)90272-0

Newport, J., Kirschner, M., 1982b. A major developmental transition in early xenopus embryos: II. control of the onset of transcription. Cell 30, 687–696. https://doi.org/10.1016/0092-8674(82)90273-2

Pritchard, D.K., Schubiger, G., 1996. Activation of transcription in Drosophila embryos is a gradual process mediated by the nucleocytoplasmic ratio. Genes & Development 10, 1131–1142. https://doi.org/10.1101/gad.10.9.1131

Rothe, M., Pehl, M., Taubert, H., Jäckle, H., 1992. Loss of gene function through rapid mitotic cycles in the Drosophila embryo. Nature 359, 156–159. https://doi.org/10.1038/359156a0

Schulz, K.N., Harrison, M.M., 2019. Mechanisms regulating zygotic genome activation. Nat Rev Genet 20, 221–234. https://doi.org/10.1038/s41576-018-0087-x

Shermoen, A.W., McCleland, M.L., O'Farrell, P.H., 2010. Developmental Control of Late Replication and S Phase Length. Current Biology 20, 2067–2077. https://doi.org/10.1016/j.cub.2010.10.021

Shermoen, A.W., O'Farrell, P.H., 1991. Progression of the cell cycle through mitosis leads to abortion of nascent transcripts. Cell 67, 303–310. https://doi.org/10.1016/0092-8674(91)90182-x

Shindo, Y., Amodeo, A.A., 2019. Dynamics of Free and Chromatin-Bound Histone H3 during Early Embryogenesis. Current Biology 29, 359-366.e4. https://doi.org/10.1016/j.cub.2018.12.020

Sibon, O.C., Stevenson, V.A., Theurkauf, W.E., 1997. DNA-replication checkpoint control at the Drosophila midblastula transition. Nature 388, 93–97. https://doi.org/10.1038/40439

Strong, I., Yuan, K., O'Farrell, P.H., 2017. Interphase-arrested embryos initiate Mid-Blastula Transition at a low nuclear-cytoplasmic ratio. bioRxiv. https://doi.org/10.1101/143719

Sung, H., Spangenberg, S., Vogt, N., Großhans, J., 2013. Number of Nuclear Divisions in the Drosophila Blastoderm Controlled by Onset of Zygotic Transcription. Current Biology 23, 133–138. https://doi.org/10.1016/j.cub.2012.12.013

Vastenhouw, N.L., Cao, W.X., Lipshitz, H.D., 2019. The maternal-to-zygotic transition revisited. Development 146, dev161471. https://doi.org/10.1242/dev.161471

Wilky, H., Chari, S., Govindan, J., Amodeo, A.A., 2019. Histone concentration regulates the cell cycle and transcription in early development. Development dev.177402. https://doi.org/10.1242/dev.177402

Yamada, S., Whitney, P.H., Huang, S.-K., Eck, E.C., Garcia, H.G., Rushlow, C.A., 2019. The Drosophila Pioneer Factor Zelda Modulates the Nuclear Microenvironment of a Dorsal Target Enhancer to Potentiate Transcriptional Output. Current Biology 29, 1387-1393.e5. https://doi.org/10.1016/j.cub.2019.03.019

Yuan, K., Seller, C.A., Shermoen, A.W., O'Farrell, P.H., 2016. Timing the Drosophila Mid-Blastula Transition: A Cell Cycle-Centered View. Trends in Genetics 32, 496–507. https://doi.org/10.1016/j.tig.2016.05.006

Figure 1

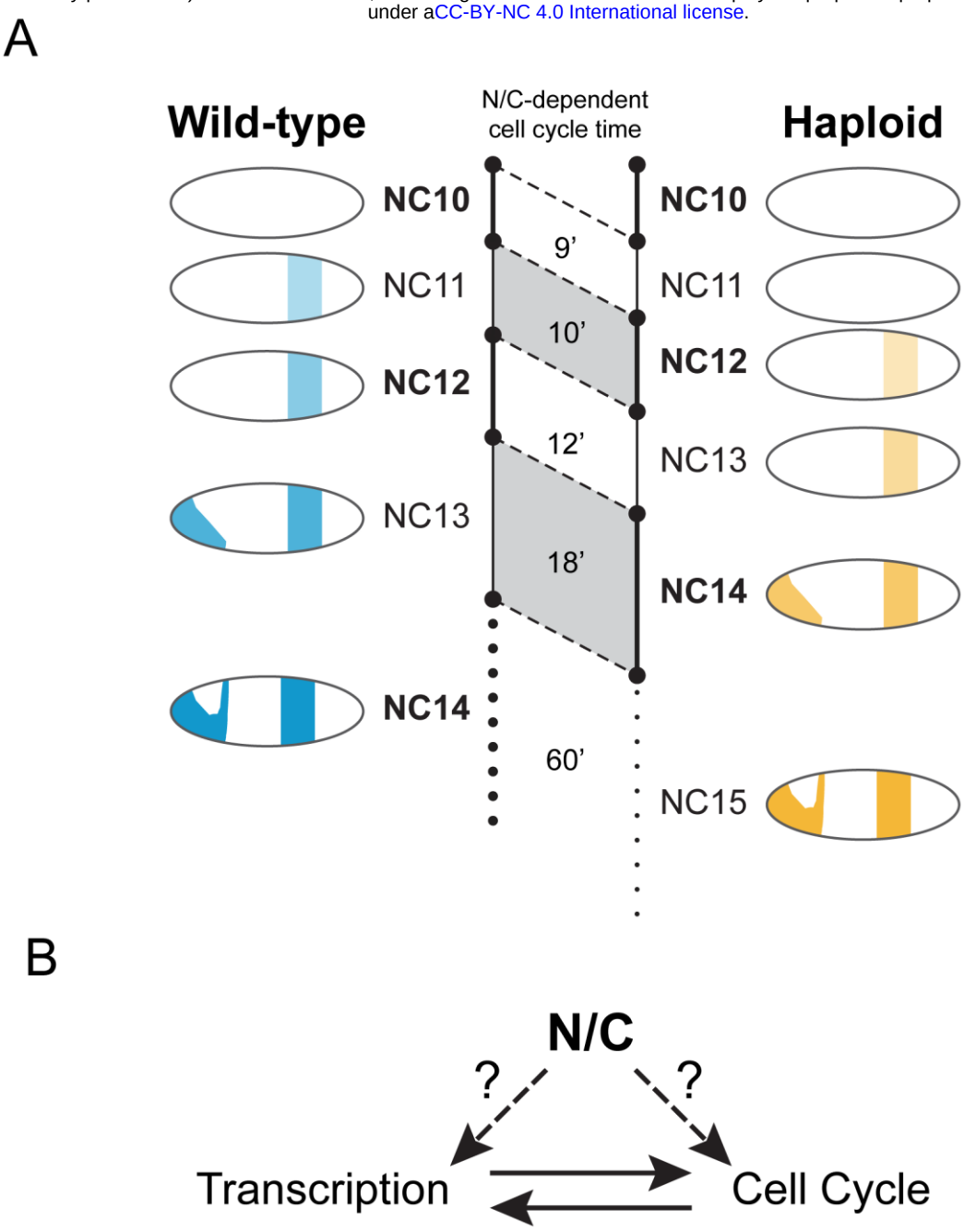

Figure 1: The Nuclear to cytoplasmic (N/C) ratio regulates cell cycle and transcription
(A) Cell cycle elongation and transcription activation (as illustrated by a cartoon of the *knirps* transcription pattern) are both delayed by reduction of the N/C ratio through reduction in ploidy. Haploid embryos undergo one additional fast cell cycle to restore the correct N/C ratio before cell cycle slowing, and all previous nuclear cycles (NCs) are correspondingly shortened (haploid NC14 is equivalent to wild-type NC13 and so on). Transcription is similarly delayed. (B) Since the N/C ratio affects both cell cycle and transcription it is difficult to disentangle which event is upstream or if both sense the N/C ratio independently. Shorter cell cycles necessarily entail less time for transcription within a given cycle.

Figure 2

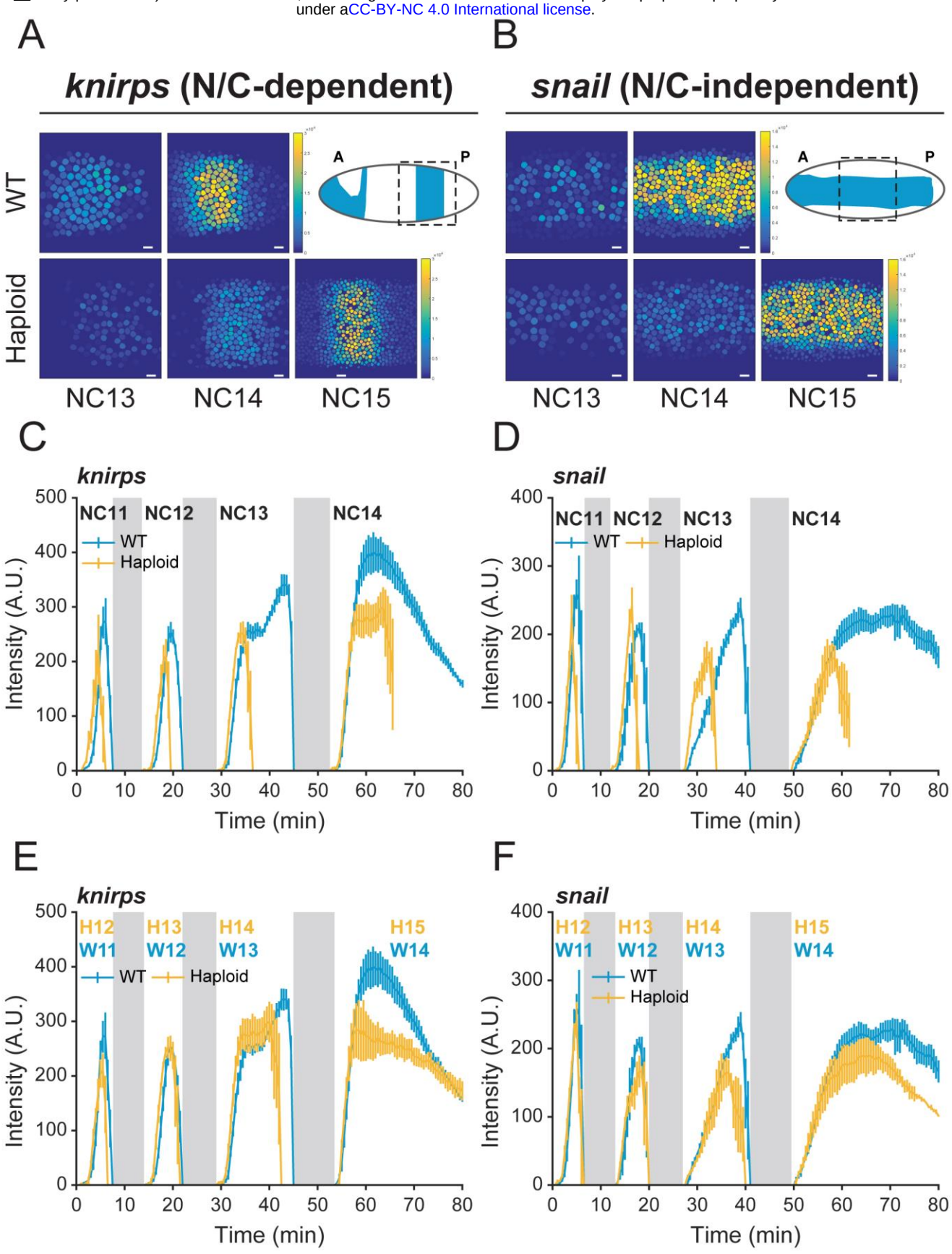

Figure 2: Total transcriptional output depends on the N/C ratio
(A) Representative images of total RNA output for previously categorized N/C-ratio-dependent gene, *kni*, in wild-type (WT) NC13-NC14 and haploid NC13-15. Color legend represents total cumulative output per nucleus per cycle (A.U.). Inset shows endogenous *kni* pattern and dotted box indicates the area under analysis. Scale bar represents 10 μm (B) Same as A except for previously categorized N/C-independent gene, *sna*. (C) Average *kni*-MS2 signal for all transcribing nuclei aligned by nuclear cycle. Haploids have shortened interphase and lower total transcriptional output compared to WT. Data represented as mean ± SEM. Grey boxes represent mitoses. (D) Same as C except for N/C-independent gene, *sna*. (E) *kni*-MS2 signal for all transcribing nuclei aligned by the N/C ratio. Data represented as mean ± SEM. Grey boxes represent mitoses. (F) Same as F except for *sna.* 6 WT and 4 haploid, and 4 WT and 3 haploid biological replicate embryos were analyzed for *kni-MS2* and *sna-MS2*, respectively.

Figure 3

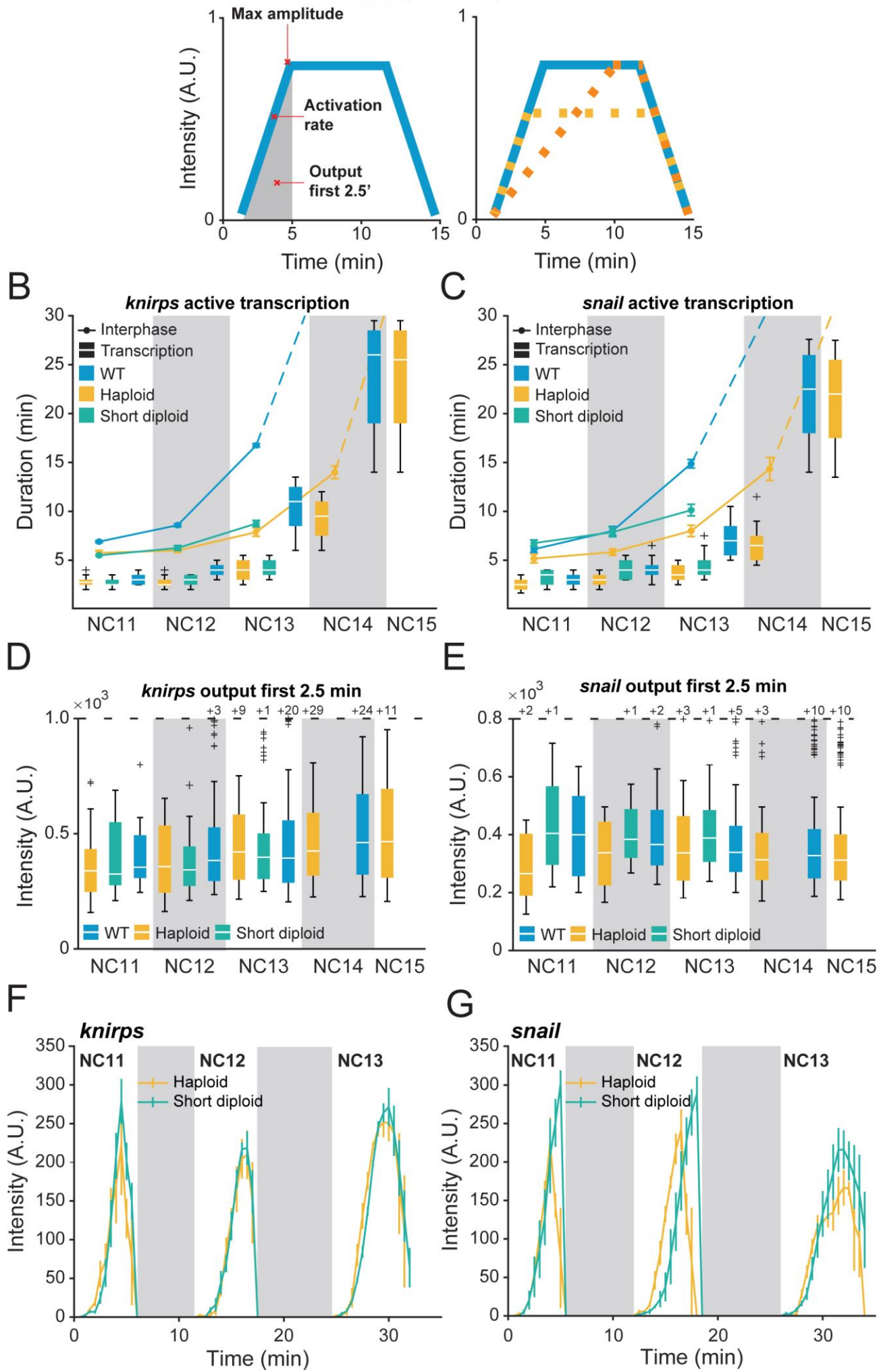

Figure 3: The N/C ratio modulates nuclear transcriptional output through cell cycle duration

(A) Schematic of different parameters that could affect transcriptional output per nucleus when controlled for cell cycle duration. If the transcriptional output post initiation was directly responsive to the N/C ratio one or more of these parameters would be changed. (B) Comparison of interphase duration (line plots) and *kni* transcription duration (boxplots) of WT (blue), haploid (yellow), and short-cycle-diploid (green) embryos. Line plots display interphase length for WT, haploid, and short-cycle-diploid embryos. Data represents mean and SEM. Dashed line corresponds to WT NC14 and haploid NC15 interphase length, which was not plotted to better highlight differences in the earlier cell cycles. Boxplots show minimum (10%), lower (25%), median, upper (75%), and maximum (90%) quantiles. Outliers are shown as '+'. (C) Same as B except for *sna*. short-cycle-diploid embryos slightly longer cell cycle duration compared to haploid, though comparable transcriptional windows. (D) Boxplots of total *kni* transcripts produced per nucleus for WT, short-cycle-diploid, and haploid embryos within the first 2.5 minutes after transcription initiation. Boxplots show minimum (10%), lower (25%), median, upper (75%), and maximum (90%) quantiles. Outliers are shown as '+'. Outliers above the dashed line were collapsed to preserve scaling of Y-axis. Number of outlier values over the cut-off are given after '+'.(E) Same as D except for *sna.* (F) Average *kni*-MS2 signal for all transcribing nuclei in haploid and short-cycle-diploid embryos. Data represent mean ± SEM. Grey boxes represent mitoses. (G) Same as F except for *sna.* 47 NC11, 184 NC12, 658 NC13, and 1051 NC14 nuclei from 6 replicate *kni-MS2* WT embryos were analyzed. 42 NC11, 121 NC12, 393 NC13, 755 NC14, and 1218 NC15 nuclei from 4 replicate *kni-MS2* haploid embryos were analyzed. 25 NC11, 68 NC12, and 267 NC13 nuclei from 4 replicate *kni-MS2* short-cycle-diploid embryos were analyzed. 109 NC11, 163 NC12, 272 NC13, and 1283 NC14 nuclei from 4 replicate *sna-MS2* WT embryos were analyzed. 58 NC11, 153 NC12, 239 NC13, 375 NC14, and 1259 NC15 nuclei from 3 replicate *sna-MS2* haploid embryos were analyzed. 146 NC11, 175 NC12, and 139 NC13 nuclei from 4 replicate *sna-MS2* short-cycle-diploid embryos were analyzed.

Figure 4

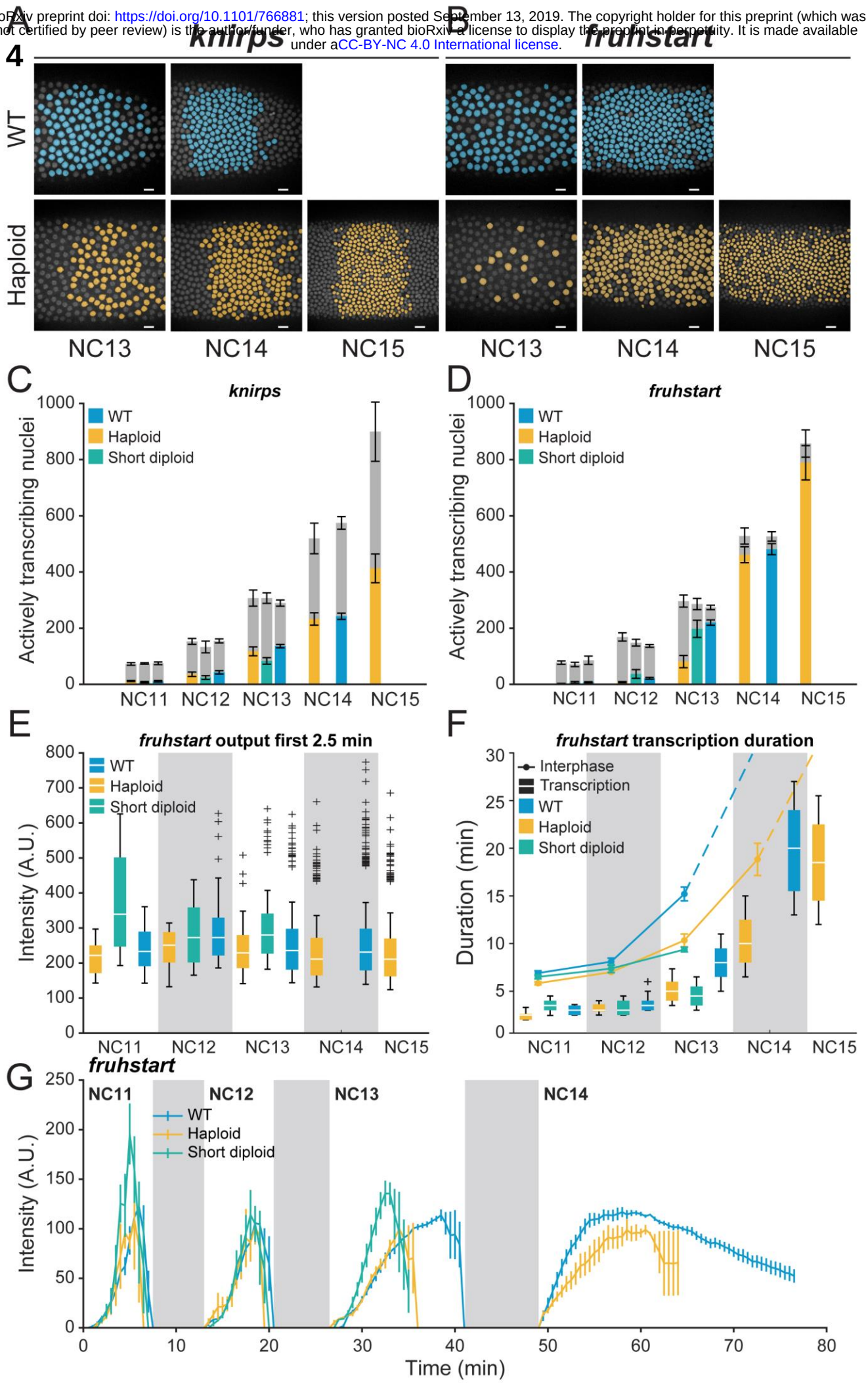

Figure 4: A subset of genes respond directly to the N/C ratio

(A) Example images where active nuclei are false colored in blue or yellow for WT and haploids respectively. Active nuclei are defined as nuclei where the total MS2 intensity crossed a threshold for more than 30% of a given cycle's duration. Scale bar represents 10 µm. (B) Same as A except for another previously defined N/C-dependent gene, *fruhstart* (*frs / Z600*). Unlike *kni*, the increase in the number of active nuclei for *frs* is delayed in haploids. (C) Plot of total active nuclei for *kni* in WT, short-cycling-diploid, and haploid embryos by cell cycle. Grey bars represent all nuclei in the frame, colored bars represent total actively transcribing nuclei. Data represented as mean ± SEM. (D) Same as C except for *frs*. (E) Boxplots of total *frs* transcripts produced per nucleus for WT, short-cycling-diploid, and haploid embryos in the first 2.5 minutes after transcription initiation. Boxplot shows minimum (10%), lower (25%), median, upper (75%), and maximum (90%) quantiles. Outliers are shown as '+'. (F) Comparison of interphase duration (line plots) and *frs* transcription duration (boxplots) of WT (blue), haploid (yellow), and short-cycling-diploid (green) embryos. Line plots display interphase length for WT, haploid, and short-cycling-diploid embryos. Data represents mean ± SEM. Dashed line corresponds to NC14 and NC15 interphase length of WT and haploid, respectively, truncated to better highlight differences in the earlier cell cycles. Boxplots of *frs* transcription duration per nucleus. Boxplot shows minimum (10%), lower (25%), median, upper (75%), and maximum (90%) quantiles. Outliers are shown as '+'. Total period of active transcription scales with interphase duration. (G) *frs*-MS2 signal for all transcribing nuclei in WT, short-cycle-diploid, and haploid embryos. Data represented as mean ± SEM. Grey boxes represent mitoses. 23 NC11, 55 NC12, 791 NC13, and 1921 NC14 nuclei from 5 replicate *frs-MS2* WT embryos were analyzed. 10 NC11, 17 NC12, 177 NC13, 1355 NC14, and 1510 NC15 nuclei from 4 replicate *frs-MS2* haploid embryos were analyzed. 24 NC11, 97 NC12, and 546 NC13 nuclei from 4 replicate *frs-MS2* short-cycle-diploid embryos were analyzed.